ANALYTICAL AND NUMERICAL PERFORMANCE ANALYSIS OF A CRYOGENIC CURRENT COMPARATOR*

N. Marsic**, W. F. O. Müller, H. De Gersem,
Institut für Theorie Elektromagnetischer Felder, Technische Universität Darmstadt, Germany
F. Kurian, T. Sieber, M. Schwickert,
GSI Helmholtzzentrum für Schwerionenforschung, Darmstadt, Germany.

Abstract

Nowadays, cryogenic current comparators (CCCs) are among the most accurate devices for measuring extremely small electric currents. This feature motivates the use of CCCs for beam instrumentation in particle accelerators. This paper presents and discusses some numerical techniques to assess the performance of such devices. In particular a 2.5D finite element model is developed. Finally, by exploiting the available numerical tools, an optimisation of the CCC geometrical dimensions is performed and analysed.

INTRODUCTION

A typical cryogenic current comparators (CCC) consists of a superconducting shield separating the current to be measured and a zero magnetic flux detector [1, 2], the latter usually being implemented by a superconducting quantum interference device (SQUID) [3]. The magnetometer is then coupled with the system through a detection coil and possibly a pickup core, as shown in Fig. 1.

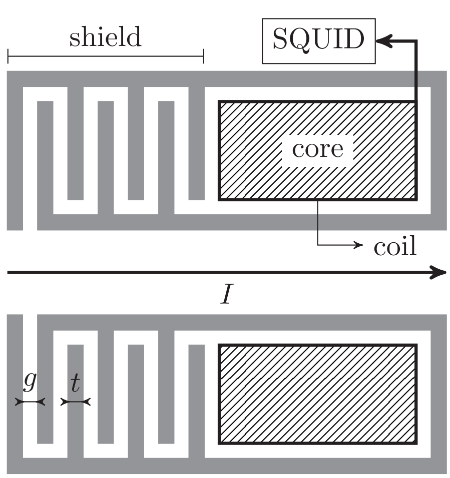

Figure 1: Scheme of a typical cryogenic current comparator (axial cut).

By choosing an appropriate shield geometry and by cooling down the device until it reaches its superconducting state, the CCC attenuates any parasitic magnetic flux, while remaining transparent to the induction field coming from the current I to be measured. This allows a precise measurement of extremely low currents, required not only for purely metrological reasons, but also for the beam diagnostic in particle accelerator facilities, such as the upcoming Facility for Antiproton and Ion Research (FAIR) in Darmstadt, Germany [4].

AVAILABLE MODELS

The topology of the CCC depicted in Fig. 1 has been deeply studied analytically in [5]. This analysis exploits the possibility to neglect contributions with an axial dependency and derives an expression for the damping provided by one meander of the shield. In the context of this paper, a meander is formed by an increasing radius ring followed by a decreasing radius ring. Eventually, the total damping exhibited by the shield is simply computed as the product of the local contributions.

Alternatively, a finite element (FE) approach can be used. The numerical setup consists of a magnetostatic model [6] in which the CCC is excited by a dipole magnetic field. The magnetic flux can then be evaluated along the shield meander structure and the damping can be assessed. It is worth mentioning that only a dipole field is needed as a source, since this field component will undergo the weakest attenuation by the shield, as predicted by theory [5]. Thus, analysing the shielding performance for a dipole field gives a relevant figure of merit.

This FE study has been successfully applied for the FAIR CCC in [7]. The geometrical data are given in Table 1 and the computed damping profile is provided in Fig. 2. The comparison of the FE solution with the analytical model shows a good accordance. However, a different behaviour can be observed for the very last meander, where the FE solution shows a significantly lower attenuation.

2.5D FINITE ELEMENT MODEL

If high precision computations are needed, a finite element approach should then be favoured. However, full three-dimensional FE simulations can be time consuming. In order to decrease this computational cost, the dimensionality of the problem can be reduced. While the geometry exhibits an axial symmetry, a full two-dimensional model cannot be constructed, since the dipole source breaks this symmetry. However, a 2.5D model can still be constructed.

* Work supported by the German Bundesministerium für Bildung und Forschung as the project BMBF-05P15RDRBB "Ultra-Sensitive Strahlstrommessung für zukünftige Beschleunigeranlagen"
** marsic@temf.tu-darmstadt.de

Table 1: Geometrical parameters

Air gap size (g)	Material thickness (t)	Inner radius	Outer radius	Meanders
0.5 mm	3 mm	120 mm	173 mm	12

The key idea of the 2.5D approach is to exploit the following harmonic decomposition:

$$B(\rho,\phi,z) = \sum_{q=-\infty}^{+\infty} B_q(\rho,z)\, e^{\jmath q\phi}, \tag{1}$$

where B is the magnetic induction vector field expressed in the cylindrical coordinate (ρ,ϕ,z) and $\jmath$ the imaginary unit. By using the magnetostatic approximation, the magnetic field can be computed by solving:

$$\mathrm{div}(\mu\,\mathrm{grad}\,\psi) = 0, \tag{2}$$

where μ is the magnetic permeability and ψ the magnetic scalar potential, defined such that $B = -\mu\,\mathrm{grad}\,\psi$ is satisfied. This Laplace equation, coupled with the decomposition (1), can be further discretized using the FE method with the following dedicated shape functions:

$$w_{i,q}(\rho,\phi,z) = N_i(\rho,z)\, e^{\jmath q\phi}, \tag{3}$$

where the $N_i(\rho,z)$ are the classical Lagrange nodal shape functions defined on a 2D mesh. Finally, the following linear system can be constructed and solved:

$$Ku + q^2 Mu = 0 \qquad \forall q, \tag{4}$$

with the matrices K and M defined as

$$\begin{aligned} K_{i,j} &= \int_V \mu\,\mathrm{grad}\,N_i(\rho,z)\cdot\mathrm{grad}\,N_j(\rho,z)\,\mathrm{d}V, \\ M_{i,j} &= \int_V \mu\frac{1}{\rho^2}\,N_i(\rho,z)\,N_j(\rho,z)\,\mathrm{d}V, \end{aligned} \tag{5}$$

where V is the computational domain and u the vector of degrees of freedom for the magnetic scalar potential. It is worth noticing that in the dipole field case, only the component $q = 1$ is relevant, Eq. (4) being thus a classical Laplace problem augmented by a diffusion term.

In order to assess the validity of this 2.5D FE model, the damping profile computed with this approach is compared to the 3D FE simulation and the analytical model discussed in the previous section. It is clear from Fig. 2 that both FE results are close to each other, validating thus the 2.5D formulation.

VOLUMETRIC OPTIMISATION

As suggested by Table 1, many parameters enter in the design of a CCC shield. For particle beam diagnostics, some parameters are fixed by external constraints:

1. the CCC inner radius (R_{in}), fixed by the beam pipe itself;

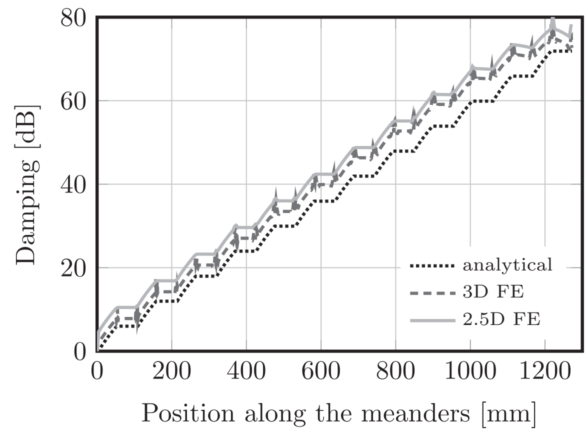

Figure 2: Damping profile for the FAIR CCC.

2. the coil cross section (S_{coil}), fixed by the measurement sensitivity;
3. the air gap size (g) and the material thickness (t), fixed by manufacturability and mechanical constraints;
4. the CCC shield damping, fixed by the electromagnetic noise level.

The values of these parameters are reported in Table 2. It is worth noticing that in the context of this optimisation work, the CCC shield damping is not a single value, but rather in a given range.

With these input data, a large set of CCCs can be designed. In order to select the best of all these candidates, the following criterion is used: the best CCC should exhibit the smallest shield volume. In order to find this best candidate, a parameter sweep is conducted. Among the free geometrical parameters, the number of meanders (N) and the outer radius (R_{out}) can be freely chosen. In the context of this work they are selected in the range: $R_{\text{out}} \in [170, 215]$ and $N \in [4, 12]$. It is worth noticing that indirectly, the number of meanders will determine the CCC shield axial length L_S:

$$L_S = 2N\,(t+g). \tag{6}$$

Then, the CCC shield volume is simply given by:

$$V_S = \pi\,(R_{\text{out}}^2 - R_{\text{in}}^2)\,L_S. \tag{7}$$

The results of the above parameter sweep are depicted in Fig. 3, which reads as follows. Each coloured dot is a realisation of the parameter sweep and its colour indicates the corresponding total damping. Encircled dots exhibit a damping in the prescribed damping range of 75 dB ±5 dB.

ISBN 978-3-95450-182-3

Table 2: Constraints for the performance comparison

Inner radius	Air gap size	Material thickness	Coil cross section	Shield damping
120 mm	0.5 mm	3 mm	60 cm^2	75 dB ±5 dB

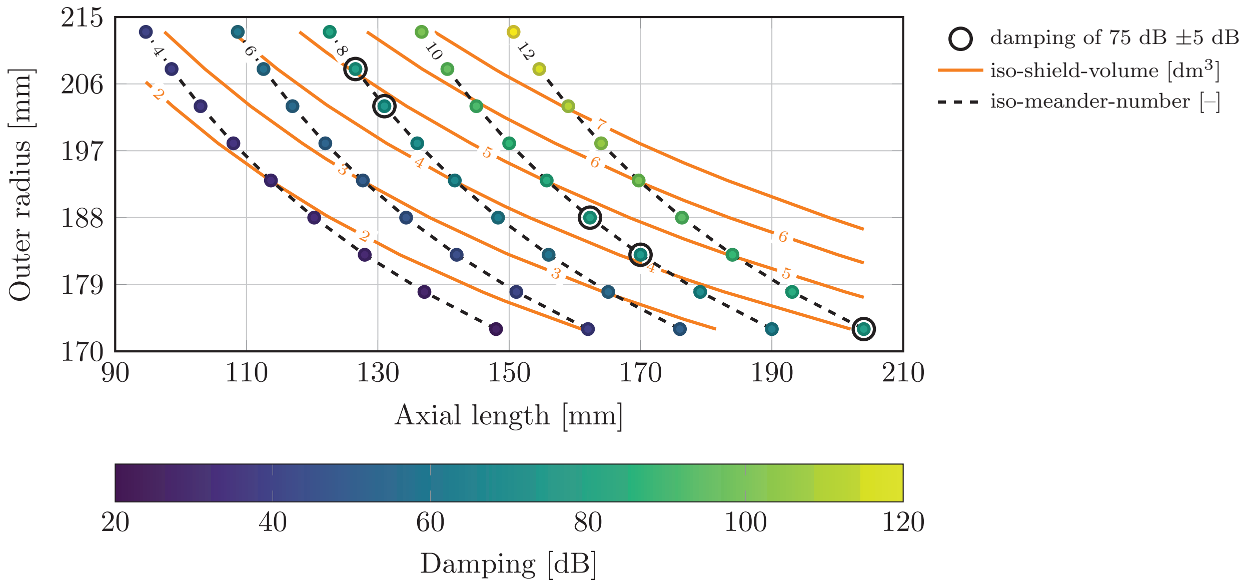

Figure 3: Shield volumetric performances for different configurations.

Dotted lines are connecting realisations with the same number of meanders and plain lines correspond to equal shield volumes.

By analysing this graph, the following conclusion can be drawn: among the parameters (outer radius and number of meanders) exhibiting the prescribed damping, the realisation with the highest number of meanders (12) and the smallest outer radius (173 mm) leads to most compact CCC shield. It is also worth mentioning that the above conclusion does not take space constraints into account, which could for instance lead to a restriction of the axial length. However, since the information is already presented as a function of the axial length, imposing an additional space constraint poses no additional difficulties.

CONCLUSION

In this work, we compared the analytical solution for the CCC damping of [5] with a magnetostatic finite element model. While both results are matching, a difference in behaviour can be noticed for the last meander. In order to decrease the cost of a full three-dimensional FE simulation, a 2.5D model is also presented and validated. By exploiting these numerical tools, a volumetric optimisation is carried out. It is found that in order to minimise the CCC shield volume, a large number of short meanders should be used. Finally, it is worth noticing that other optimisation criteria could be used in place of the volumetric one. Among these, a weight optimisation is also a meaningful candidate.

REFERENCES

[1] I. K. Harvey, "A precise low temperature dc ratio transformer," *Review of Scientific Instruments*, vol. 43, no. 11, pp. 1626–1629, 1972.

[2] J. M. Williams, "Cryogenic current comparators and their application to electrical metrology," *IET Science, Measurement and Technology*, vol. 5, no. 6, pp. 211–224, 2011.

[3] R. L. Fagaly, "Superconducting quantum interference device instruments and applications," *Review of Scientific Instruments*, vol. 77, no. 10, 2006.

[4] R. Geithner, W. Vodel, R. Neubert, P. Seidel, F. Kurian, H. Reeg, and M. Schwickert, "An improved cryogenic current comparator for FAIR," in *3rd International Particle Accelerator Conference IPAC'12*, pp. 822–824, 2012.

[5] K. Grohmann, H. D. Hahlbohm, D. Hechtfischer, and H. Lübbig, "Field attenuation as the underlying principle of cryo-current comparators 2. Ring cavity elements," *Cryogenics*, vol. 16, no. 10, pp. 601–605, 1976.

[6] A. Bossavit, *Computational electromagnetism: variational formulations, complementarity, edge elements*. Academic Press, 1998.

[7] F. Kurian, *Cryogenic current comparators for precise ion beam current measurements*. PhD thesis, Johann Wolfgang Goethe-Universität Frankfurt am Main, Deutschland, 2016.